Article

Anion Exchange Membrane Reinforced with Polyethylene Substrate for Alkaline Fuel Cell Applications

Ahmed Mohamed Ahmed Mahmoud [1,2], Keijiro Nagahara [3] and Kenji Miyatake [1,4,5,*]

[1] Clean Energy Research Center, University of Yamanashi, Kofu 400-8510, Japan; ammedo@yamanashi.ac.jp

[2] Chemistry Department, Faculty of Science, Sohag University, Sohag 82524, Egypt

[3] Interdisciplinary Graduate School of Medicine and Engineering, University of Yamanashi, Kofu 400-8510, Japan; g22ta022@yamanashi.ac.jp

[4] Fuel Cell Nanomaterials Center, University of Yamanashi, Kofu 400-0021, Japan

[5] Department of Applied Chemistry, Waseda University, Tokyo 169-8555, Japan

* Corresponding author. E-mail: miyatake@yamanashi.ac.jp

ABSTRACT: To enhance mechanical robustness of our in-house anion exchange membrane (QPAF-4), the reinforcement technique was applied using ozone-treated, porous polyethylene (PE) thin film (Toray SETELA) as a substrate. Homogenous and flexible reinforced membranes (QPAF-4-PE, 15–20 μm thick) were obtained by bar-coating method. The cross-sectional SEM image and EDS analysis revealed triple-layered (sandwich-like) structure without detectable pinholes. The QPAF-4-PE with ion exchange capacity (IEC) of 1.48 meq·g^{-1} exhibited lower water uptake (15 wt% at 90% relative humidity) and slightly lower hydroxide ion conductivity (71 mS·cm^{-1} at 80 °C) than those of the pristine QPAF-4 (IEC = 1.84 meq·g^{-1}, 25 wt% water uptake and 82 mS·cm^{-1} of the conductivity). The reinforced QPAF-4-PE exhibited slightly higher viscoelasticity (particularly, in MD direction) due to the suppressed water absorbability. Furthermore, the elongation at break increased by 9.8% in TD direction and 6.3% in MD direction. An H$_2$/O$_2$ fuel cell using QPAF-4-PE as membrane was investigated at different back-pressure, in which the cell with 100 kPa back-pressure onto the cathode side only achieved the maximum performance (176 mW·cm^{-2} at current density of 364 mA·cm^{-2}) and the longest durability for (>200 h) at a constant current density of 100 mA·cm^{-2} maintaining 0.43 V of the cell voltage (67% remaining). The durability was eight times longer than that with ambient pressure and two times longer than that with back-pressure on both sides.

Keywords: Reinforced composite membranes (RCMs); Anion exchange membranes; Hydroxide ion conductivity; Alkaline stability; Alkaline fuel cells; In-situ durability

1. Introduction

The global warming and the increasing demand to eliminate the fossil fuels, have motivated the scientists to look for alternative resources for clean energy [1,2]. Fuel cells are one of the most attractive energy conversion devices to produce clean energy. Anion exchange membrane fuel cells (AEMFCs) have attracted the increasing interest in the last decade owing to the possible utilization of abundant non-platinum group metals (NPGMs) as electrocatalysts. Furthermore, the alkaline medium for AEMFCs offers other advantages such as use of inexpensive bipolar plates and liquid fuels (e.g., hydrazine hydrate and borates) [3,4]. AEMs for FCs are required to have multi-functions such as gas separation, ion and water transportation, and binding catalyst particles in the catalyst layers. The overall properties of AEMs often determine the fuel cell performance [5]. Longevity associated with chemical instability and low mechanical strength remains issues for AEMs, restricting commercialization of AEMFCs.

A great number of efforts have been devoted to develop alkaline stable and mechanically robust AEMs. Major advances have been achieved by utilizing ether-free polymer backbones [6] and/or by manipulating the quaternary ammonium structure [7–10]. We produced an alkaline stable AEM (4-QPPAF-TMA) that survived for 1000 h in 8 M KOH at 80 °C without losses in conductivity and mechanical properties [11]. Imidazolium-based AEM was reported to be stable for 2400 h in 10 M KOH at 80 °C [12,13]. Hibbs et al. developed benzyl trimethylammonium-type polyphenylene-based AEMs with six-carbon spacer that showed 5% loss in conductivity when tested in 4 M KOH at 90 °C for 336 h [14]. A series of side chain type terphenylene-based AEMs with pendent piperidinium cations survived for 720 h in 2 M NaOH at 90 °C with <5% degradation [15]. Fluorene polymer-based AEMs exhibited excellent stability in 1 M NaOH at 80 °C for 30 days [16].

Compared with the progress in alkaline stability, mechanical strength of ether-free AEMs needs more improvement [17–20]. Most of the above mentioned alkaline stable AEMs suffered from low mechanical properties. For example, QPPAF-TMA membrane had low elongation properties (16 MPa tensile strength (TS) and 32% elongation at break (EB)) [11]. The rigid imidazolium-based AEMs exhibited reasonable TS (57.2–75.0 MPa) but showed low EB (17.4–28.7%) [12].

Reinforcement with porous, non-ionic substrate seems effective approach for enhancing the mechanical robustness of AEMs [21–24]. For example, Wang et al. reported that reinforced composite membranes (RCMs) composed of poly(fluorenyl-co-terphenyl piperidinium) and polyethylene (PE) porous substrate possessed enhanced mechanical properties (110 MPa TS and 75% EB) compared to those (68.0 MPa TS and 30% EB) of the non-reinforced membrane [21]. Chuan et al. developed poly(aryl-co-aryl piperidinium)-based RCMs with PE substrate that exhibited excellent mechanical properties (~114 MPa TS and ~159% EB) maintaining its chemical and mechanical durability even after fuel cell testing at current density of 0.6 A·cm^{-2} and 70 °C for ~ 360 h [22]. Recently, we reported that robust and stable imidazolium-based RCMs using plasma treated porous PE substrate exhibited reasonable mechanical strength (24 MPa TS and 205% EB), compared to brittle and cracked non-reinforced ionomer membrane [23].

In the present work, RCM was prepared from our partially fluorinated, pendent ammonium type AEM (QPAF-4) [25] and porous PE substrate. Effect of reinforcement on membrane properties such as morphology, water absorbability, ion conductivity and mechanical robustness was carefully investigated. Furthermore, the performance of an H$_2$/O$_2$ fuel cell and in-situ durability under different backpressure conditions were also elucidated.

2. Materials and Methods

2.1. Materials

Quaternized copolymers (QPAF-4) were synthesized according to the literature [25]. A porous polyethylene substrate (SETELA PE7: thickness = 7 μm, porosity = 44% and pore size = 62 nm) was kindly supplied by Toray and pre-treated with ozone/UV surface treatment system (EKBIO-1100, Ebara Jitsugyo CO. LTD., Kisarazu, Japan) for 60 min prior to use.

2.2. Preparation of Reinforced QPAF-4-PE Membranes

The reinforced membranes were prepared using bar coat applicator (SA-204, Tester Sangyo Co. Ltd., Miyoshi, Japan) with constant coating speed (5 mm·s^{-1}). A detailed procedure is as follows:

Quaternized QPAF-4 copolymer [25] was dissolved in DMAc (18 wt%) with stirring at 40 °C. A polypropylene (PP) sheet (AS ONE co., Osaka, Japan) was fixed on a flat glass plate heated at 70 °C. The QPAF-4 solution was spread onto the PP sheet surface using the bar coat applicator. A porous PE substrate was placed on the copolymer solution using the applicator. Another portion of the copolymer solution was spread over the porous PE substrate. The multilayered membrane was dried at 70 °C for 12 h to ensure full impregnation of the copolymer into the PE substrate. A flexible and transparent membrane in dimethyl sulfate ion form (QPAF-4-PE) was obtained with adjustable thickness of 15–20 μm. The PP sheet was peeled off prior to use.

2.3. Ion Exchange Reaction

2.3.1. Hydroxide Ion Form

The QPAF-4-PE membrane in hydroxide ion form was obtained by immersing the sample in 1 M KOH at 80 °C for 48 h. The samples were washed with degassed ultrapure water several times to remove any residual KOH.

2.3.2. Chloride Ion Form

The QPAF-4-PE in chloride ion form was obtained by immersing the samples (in OH$^-$ form) in 2 M NaCl solution for 24 h. The samples were washed with degassed ultrapure water several times and dried under vacuum at 60 °C.

2.4. Membrane Characterization

The detailed procedure for the membrane characterization including titration (for ion exchange capacity), scanning electron microscopy (SEM), transmission electron microscopy (TEM), hydroxide ion conductivity, universal stress-strain (S-S) curves, and dynamic mechanical analyses (DMA) was described in our previous works [11,23,25–27].

2.4.1 Water Uptake

Humidity dependence of water uptake of the parent QPAF-4 and reinforced QPAF-4-PE membranes was measured at 60 °C with a vapor sorption analyzer system (VSTAR, Quantachrome Instruments Co., Boynton Beach, FL, USA) in a humidity-controllable chamber. The quantitative adsorption of vapor as a function of relative humidity was measured. The dry weight of the sample was measured by a magnetic suspension balance then the samples were exposed to a given humidity for at least 2 h providing the wet weight. The water uptake (WU, %) was calculated from the following equation:

$$WU = [(\text{wet weight} - \text{dry weight})/\text{dry weight}] \times 100$$

2.4.2. Preparation of Gas Diffusion Electrodes (GDEs) and Membrane Electrode Assembly (MEA)

A modified procedure from our previous work was adopted [23]. A catalyst paste was prepared from QPAF-4 (IEC = 2.0 meq·g^{-1} in HCO$_3^-$ form) [25] as the electrode binder and 50 wt% Pt-loaded catalyst (Pt/CB, TEC10E50E, Tanaka Kikinzoku Kogyo, Tokyo, Japan) as the electrocatalyst. The catalyst was suspended in methanol/ultra-pure water using a planetary ball mill for 30 min. Then, 5 wt% QPAF-4 solution in MeOH was added to the catalyst slurry. The mixture was homogenized using a planetary ball mill for further 30 min. The ratio of dry binder to carbon black was adjusted to be 0.7 by weight. The catalyst paste was sprayed onto a gas diffusion layer (GDL, 29BC, SGL Carbon Group Co., Ltd., Wiesbaden, Germany) using a pulse-swirl-spray apparatus to form a gas diffusion electrode (GDE) with Pt loading of 0.25 ± 0.02 mg·cm^{-2} for both electrodes and active geometric area of 4.41 cm^2. The reinforced membrane (QPAF-4-PE, IEC = 1.48 meq·g^{-1})) and two GDEs were immersed in 1.0 M KOH for 48 h at 80 °C. The membrane was sandwiched by the two GDEs and the resulting MEA was mounted into a single cell consisting of two carbon separator plates. The fuel cell was operated at 60 °C and 75% RH for anode and 100% RH for cathode, respectively. The flow rate of H$_2$ and O$_2$ was adjusted at 100 mL·min^{-1}. The high-frequency resistance (HFR) was measured using Kikusui FC impedance analyzer at 6.0 kHz.

2.4.3. Durability Test

The durability of the reinforced QPAF-4-PE membrane was carried out at 60 °C at constant current density of 100 mA·cm^{-2}. The cell voltage was monitored for 220 h.

3. Results and Discussion

3.1. Preparation of Reinforced QPAF-4-PE Membrane

The quaternized QPAF-4 copolymer (IEC = 1.84 meq·g^{-1}) (Figure 1) was synthesized from 1,6-bis(3-chlorophenyl)perfluorohexane and 6,6′-(1,7-dichloro-9H-fluorene-9,9-diyl)bis(N,N-dimethylhexan-1-amine) via Ni(0)-promoted polycondensation reaction according to our previous work [25]. Although QPAF-4 copolymer membranes were mechanically robust, the reinforcement technique was applied for further improving the mechanical properties using 18 wt% copolymer in DMAc and porous polyethylene (PE) film (SETELA) as a substrate. The hydrophilicity and ionomer compatibility of the PE substrate were enhanced by ozone surface treatment for 60 min prior to use. The contact angel of water decreased from 98.9° to be 70.5° after 10 min UV treatment and 66.5° after 60 min treatment suggesting enhanced hydrophilicity. The reinforced membrane was prepared by a modified procedure of the reported push-coat method [23,28] in which QPAF-4 solution was sprayed onto both sides of the pretreated PE substrate with the help of applicator and bar coater (Figure 2). The applicator and bar coater were crucial for the reinforced membranes with flatness and controllable thickness (Figure S1).
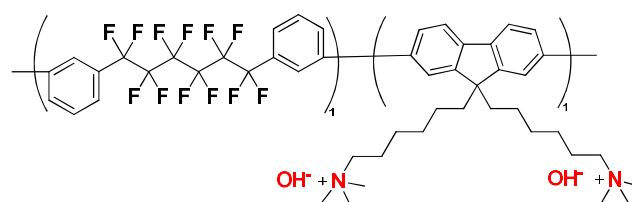

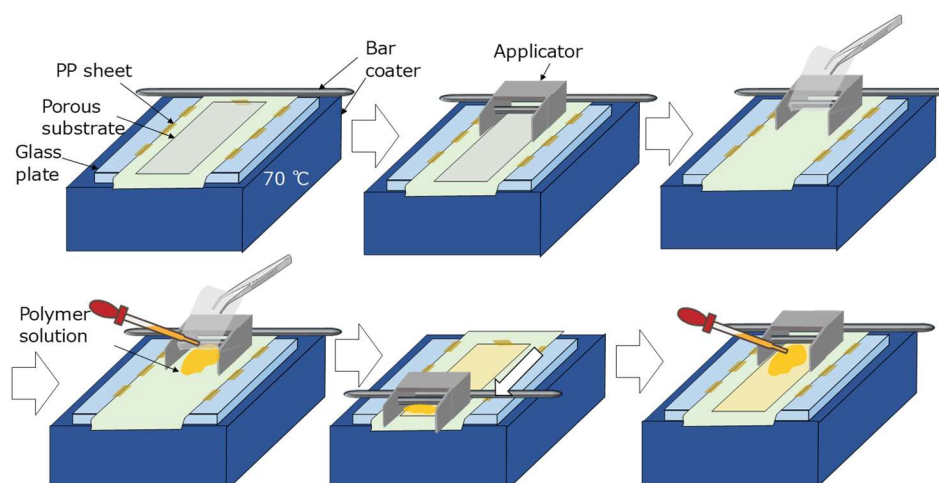**Figure 1.** Chemical structure of QPAF-4 copolymer.

Figure 2. Schematic diagram of the reinforcement process using applicator.

The resulting reinforced membrane (QPAF-4-PE) was homogeneous and flexible with 15–20 μm in thickness (Figure 3). Compared to the PE substrate which was white and not transparent, QPAF-4-PE was light brown and transparent indicating impregnation of the ionomer into the pores of the PE substrate (when the impregnation was not complete, the resulting membranes remained white or turbid).
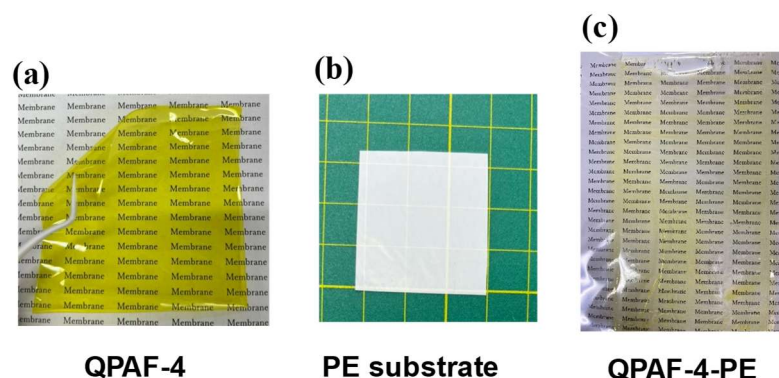

Figure 3. Photos of (**a**) QPAF-4 pristine membrane, (**b**) SETELA porous PE substrate and (**c**) reinforced QPAF-4-PE membrane.

3.2. Morphology

The morphology of the reinforced QPAF-4-PE membrane was investigated through cross-sectional scanning electron microscopy (SEM) image (Figure 4a) revealing a triple-layered (sandwich-like) structure (i.e., QPAF-4/QPAF-4-PE/QPAF-4). The upper (air side) and lower (PP side) layers were composed of QPAF-4 ionomer (ca. 6.2 and 3.2 μm thick, respectively) without PE substrate. The middle layer (ca. 6.2 μm thick) was the composite of QPAF-4 and PE substrate, in which no pores and cracks were detected suggesting successful pore-filling in the PE substrate with QPAF-4 ionomer. The average thickness of the composite membrane measured from the SEM image was ca. 16.6 μm that was in accordance with the micrometer thickness (15–20 μm). The lower layer exhibited smaller thickness compared to the upper layer because the PE substrate sank under the compression applied from the applicator during the impregnation process. The energy-dispersive X-ray spectrum (EDS) confirmed the above triple-layered structure (Figure 4b). The fluorine atom intensity in the upper and bottom layers (pure QPAF-4 layers) was significantly higher than that in the middle layer (QPAF-4-PE), where the ratio of the maximum fluorine intensity in the middle layer to those in the upper and lower layers was 50%, in fair agreement with the porosity of PE substrate (44%). The titrated ion exchange capacity (IEC_{tit}) of the QPAF-4-PE membrane was 1.48 meq·g^{-1}, that was higher than the calculated IEC (1.24 meq·g^{-1}) from the IEC of the pristine QPAF-4 copolymer (1.84 meq·g^{-1}) and the porosity (44%) of the PE substrate due to the pure ionomer layer on both sides of the composite layer.

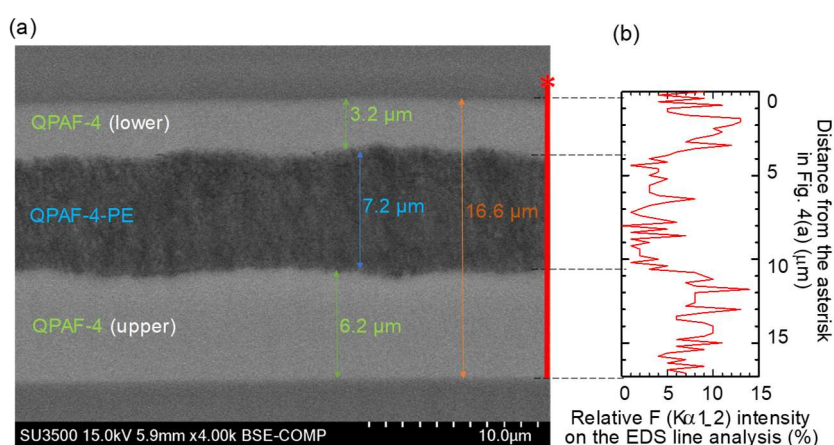**Figure 4**. (**a**) Cross-sectional SEM image of QPAF-4-PE reinforced membrane. (**b**) Relative fluorine atom (Kα1_2) intensity on the EDS line analysis (%) as a function of the distance from asterisk in panel a (μm).

3.3. Water Absorbability

One of the main objectives of the reinforcement is to suppress excess swelling (water absorbability) of AEMs under humidified conditions, simulating operating fuel cells. Thus, the water uptake of QPAF-4-PE membrane (in CH$_3$SO$_3^-$ ion form) was measured using vapor sorption analyzer as a function of the relative humidity (RH%) at constant temperature (60 °C) (Figure 5). Notably, the reinforced QPAF-4-PE membrane exhibited lower water uptake compared to that of the pristine QPAF-4 membrane, in particular, at high humidity due to the hydrophobic PE-substrate. The maximum water uptake of the reinforced QPAF-4-PE was 15 wt% at 90% RH compared to 25 wt% of the pristine membrane. Furthermore, the dimensional change of the reinforced membrane was

measured as a function of temperature (Figure S2) in which the reinforced membrane showed smaller swelling (9.9–12.9% at 30–60 °C) compared to (25.0–31.5%) for the pristine QPAF-4 membrane. The results confirm that the hydrophobic PE substrate contributed to suppressing the water absorbability of the QPAF-4 membrane.
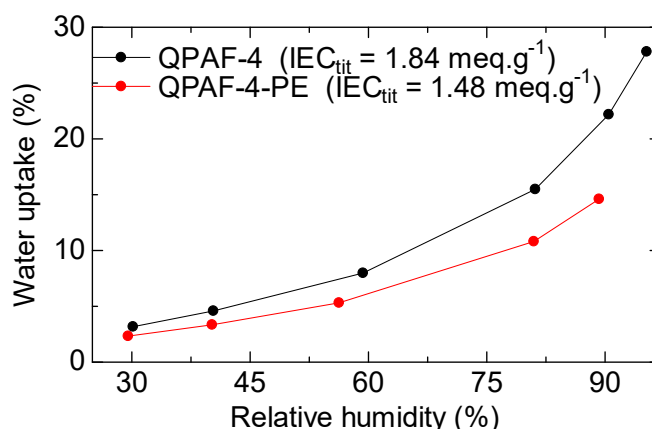

Figure 5. Water uptake of QPAF-4 and QPAF-4-PE membranes at 60 °C as a function of the relative humidity.

3.4. Hydroxide Ion Conductivity

Temperature dependence of hydroxide ion conductivity of QPAF-4-PE membrane (IEC = 1.48 meq·g^{-1}) was measured in water and compared to that of the pristine QPAF-4 (IEC = 1.84 meq·g^{-1}) (Figure 6). Because of the lower IEC, the reinforced QPAF-4-PE membrane exhibited slightly lower conductivity (37 mS·cm^{-1} at 30 °C and 71 mS·cm^{-1} at 80 °C) compared to that (45 mS·cm^{-1} at 30 °C and 82 mS·cm^{-1} at 80 °C) of the pristine QPAF-4 membrane. The apparent activation energies (E_a) for the hydroxide ion conduction were estimated from the slopes to be E_a = 11.4 kJ·mol^{-1} and 10.3 kJ·mol^{-1} for the reinforced and pristine membranes, respectively, suggesting that the PE substrate did not affect the hydroxide ion conduction mechanism.
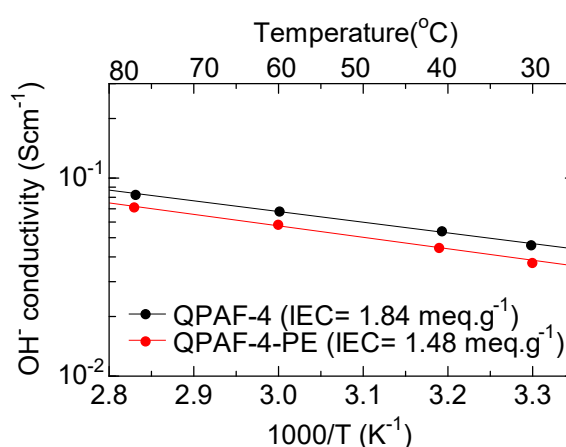

Figure 6. Temperature dependence of hydroxide ion conductivity of QPAF-4 and QPAF-4-PE membranes.

3.5. Mechanical Properties

The viscoelastic properties of QPAF-4-PE membrane in machine direction (MD) and transverse direction (TD) were measured by DMA analysis as a function of temperature (at 60% RH, Figure 7a) and humidity (at 80 °C, Figure 7b). At 60% RH, QPAF-4-PE membrane exhibited higher initial values of the storage modulus (E′), loss modulus (E″) and tan δ (= E″/E′) compared to those of the pristine QPAF-4 but lower than those of PE-SETELA (MD), presumably reflecting the water absorbability (see Figure 5). As expected, QPAF-4-PE exhibited slightly higher viscoelasticity in MD direction than in TD direction. The broad peak associated with the glass transition (T_g) was observed at 55 °C for PE-SETELA (MD) and 65 °C for both QPAF-4-PE and pristine QPAF-4. It is noted that the reinforced QPAF-4-PE retained higher E′ and E″ values than those of the pristine membrane above T_g due to the suppressed water absorbability. In the humidity dependence, the differences in E′ and E″ of QPAF-4-PE (MD) and (TD) were smaller. A broad but not distinctive peak was observed in tan δ curves at ca. 45% RH for QPAF-4-PE membrane. At higher humidity, the values of E′, E″ and tan δ of QPAF-4-PE were less dependent on the humidity that those of the pristine QPAF-4. PE-SETELA (MD) exhibited viscoelastic properties independent on the humidity without detectable peaks. The results reveal that compositing QPAF-4 with PE substrate contributed to suppressing the water absorbability and accordingly, improving the viscoelastic properties.
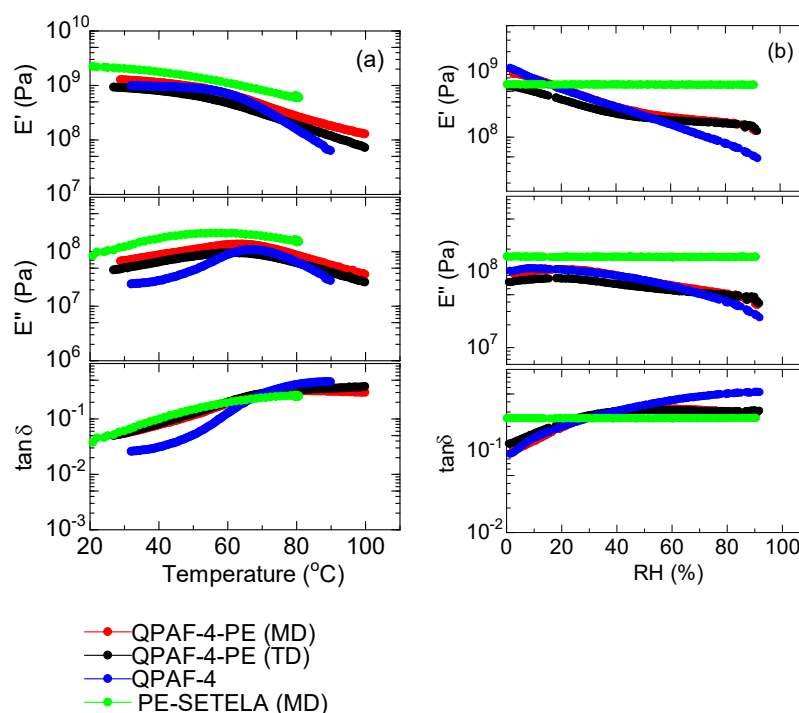
Figure 7. DMA analyses of QPAF-4, QPAF-4-PE, and porous PE substrate membranes as a function of (**a**) temperature (°C) and (**b**) humidity (RH%).

The elongation properties of the reinforced QPAF-4-PE membrane in MD and TD directions were tested through the stress-strain curves (Figure 8). The reinforced QPAF-4-PE exhibited slightly higher elongation (220% for TD direction and 213% for MD direction) compared to 204 % for the pristine QPAF-4. It is noted that the elongation properties were similar in TD and MD direction for QPAF-4-PE membrane while the porous PE substrate exhibited large differences between TD (52 MPa and 407% for the maximum stress and strain) and MD (141 MPa and 225% for the maximum stress and strain) directions (Figure S3). The results suggest that the elongation properties were rather dominated by the ionomers and thus, the reinforcement effect on QPAF-4 with PE substrate was minor.
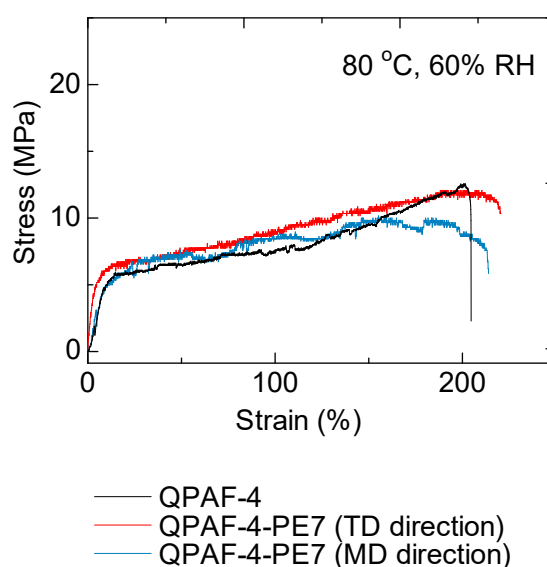

Figure 8. Stress-strain curves of QPAF-4 and QPAF-4-PE membranes in machine and transverse directions.

3.6. Fuel Cell Performance

Alkaline fuel cell performance was investigated using the reinforced QPAF-4-PE (IEC = 1.48 meq·g^{-1}) as membrane and in-house QPAF-4 (IEC = 2.0 meq·g^{-1}) as electrode binder with Pt/C (loading amount of Pt was 0.25 mg·cm^{-2}) as catalyst for both anode and cathode. The fuel cell performance was measured at different back pressure as shown in Figure 9. In all cases, the OCV was as high as 0.98–1.02 V indicating gas impermeability of the QPAF-4-PE membrane even under the pressurized conditions. At ambient pressure (without back pressure), the cell achieved peak power density (PPD) of 125 mW·cm^{-2} at current density of 250 mA·cm^{-2}. With increasing the back pressure to 250 kPa at both anode and cathode sides, the performance decreased to PPD of 88

mW·cm^{-2} at current density of 182 mA·cm^{-2}. Detailed performance at different back pressure on both sides is shown in Figure S4 in which the performance decreased and ohmic resistances increased as the back pressure gradually increased. It seems that applying back pressure at anode side had a negative impact on the performance presumably due to the flooding of liquid water in the anode. Thus, the back pressure of 100 kPa was applied to the cathode side only (higher pressure was avoided for safety and to circumvent membrane cracking), in which the performance increased significantly to reach PPD of 176 mW·cm^{-2} at current density of 364 mA·cm^{-2}, suggesting that cathode back pressure suppressed the cathode dry-out by maintaining water in the cathode layer. Under the same back pressure conditions (100 kPa at cathode), the oxygen was exchanged with air in which the PPD decreased to 125 mW·cm^{-2} at current density of 273 mA·cm^{-2} due to the higher flow rate of the air to blow out the water. The ohmic resistance of the cells was higher when the back pressure was applied onto the cathode side only (Figure S5). Then, IR-free and IR-included cell voltages were plotted as a function of the current density under different back pressure conditions (Figure S6), in which the differences in performance of IR-free and IR-included became larger by applying back pressure onto the cathode side, reflecting higher ohmic resistance.

The pristine QPAF-4 achieved peak power density of 340 mW·cm^{-2} at current density of 780 mA·cm^{-2} that was two times higher than that of the reinforced QPAF-4-PE membrane presumably due to better compatibility of the former membrane with the catalyst layer [29].
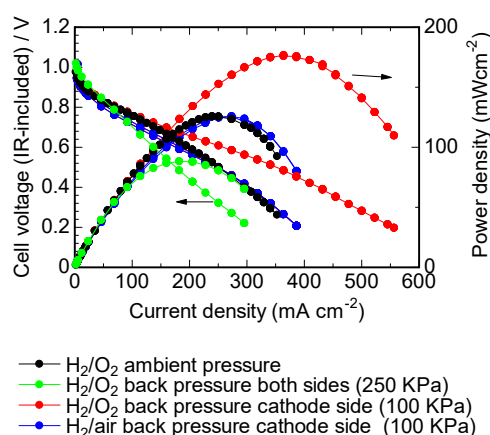

Figure 9. Fuel cell performance of QPAF-4-PE membrane under different back pressure conditions.

The durability test was performed at constant current density of 100 mA·cm^{-2} and different back pressure conditions in which the cell voltage and ohmic resistance were monitored (Figure 10). At ambient pressure, the cell survived for 107 h maintaining 0.23 V and 31% of initial voltage. By applying 175 kPa of the back pressure on both sides of the electrodes, the cell encountered fourfold decrease in durability, in which the cell survived for only 26 h maintaining 0.29 V and 32% of initial voltage. The cell survived much longer time (> 200 h) when 100 kPa of the back pressure was applied onto the cathode side only, maintaining 0.43 V and 67% of initial voltage, which was eight times longer than that with ambient pressure and two times longer than that with both sides back pressure. The ohmic resistance slightly increased under any conditions, indicating that the performance degradation would be related more with the catalyst layers. Compared to the pristine QPAF-4 membrane that was tested at constant current density of 20 mA·cm^{-2} with average decay of 244 μV·h^{-1} [25], the reinforced QPAF-4-PE was more durable to survive at 5 times higher current density (100 mA·cm^{-2}).
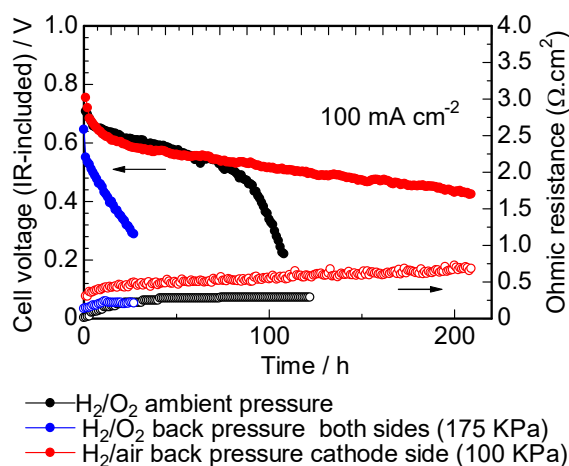

Figure 10. Durability of the fuel cells using QPAF-4-PE membrane at constant current density of 100 mA·cm^{-2} and 60 °C under different back pressure conditions.

4. Conclusions

Partially fluorinated, quaternized copolymer (QPAF-4) was reinforced with commercially available porous polyethylene (PE) substrate. Using a bar coater, homogenous and flexible composite membrane was obtained with controllable thickness. Cross-sectional SEM images revealed triple-layered structure, where QPAF-4 ionomer was fully impregnated into PE substrate in the middle layer. The cross-sectional fluorine content in the EDS analysis further supported the triple-layered structure of the composite membranes. The reinforced QPAF-4-PE membrane exhibited lower IEC (1.48 meq·g^{-1}) compared to 1.84 meq·g^{-1} of the pristine QPAF-4. The reinforcement effect was confirmed in the suppressed water absorbability and improved viscoelastic properties. The elongation properties of the reinforced QPAF-4-PE membranes did not reflect the differences in TD and MD direction of the original porous substrate, but exhibited isotropic behavior. The reinforced QPAF-4-PE membranes was tested in fuel cells under different back pressure conditions. In spite of higher ohmic resistance, applying the back pressure onto the cathode side contributed to maintaining the cathode side wet and in turn significantly improved the fuel cell performance and in-situ durability. In contrast, the ambient and both sides pressurized conditions resulted in unbalanced water and thus, lower performance and durability. The slight change in the ohmic resistance during the durability test revealed that the major degradation would be associated with catalyst layer rather than reinforced membrane.

Supplementary Materials

The following supporting information can be found at: https://www.sciepublish.com/article/pii/72. Figure S1: Photos of bar coater and applicator used in the reinforcement process; Figure S2: Stress-strain curves of PE porous substrate; Figure S3: Ohmic resistance of QPAF-4-PE membrane at different fuel cell operating conditions; Figure S4: IR-free and IR-included polarization curves of QPAF-4-PE membrane under different back pressure conditions; Figure S5: Ohmic resistance of the fuel cells using QPAF-4-PE membrane under different back pressure conditions; Figure S6: IR-free and IR-included polarization curves of the fuel cells using QPAF-4-PE membrane under different back pressure conditions.

Author Contributions

Conceptualization, A.M.A.M. and K.M.; Methodology, A.M.A.M. and K.N.; Software, A.M.A.M. and K.N.; Validation, K.M.; Formal Analysis, A.M.A.M. and K.N.; Investigation, A.M.A.M. and K.N.; Resources, K.M.; Data Curation, A.M.A.M.; K.N. and K.M.; Writing—Original Draft Preparation, A.M.A.M.; Writing—Review & Editing, K.M.; Visualization, A.M.A.M. and K.N.; Supervision, K.M.; Project Administration, K.M.; Funding Acquisition, K.M.

Ethics Statement

Not applicable.

Informed Consent Statement

Not applicable.

Funding

Declaration of Competing Interest

The authors declare no competing interest.

References

1. Mandal M. Recent advancement on anion exchange membranes for fuel cell and water electrolysis. *Chemelectrochem* **2020**, *8*, 36–45.
2. Feng Z, Gupta G, Mamlouk M. A review of anion exchange membranes prepared via Friedel-Crafts reaction for fuel cell and water electrolysis. *Int. J. Hydrog. Energy* **2023**, *48*, 25830–25858.
3. Proch S, Stenström M, Eriksson L, Andersson J, Sjöblom G, Jansson A, et al. Coated stainless steel as bipolar plate material for anion exchange membrane fuel cells (AEMFCs). *Int. J. Hydrog. Energy* **2020**, *45*, 1313–1324.
4. Hren M, Božič M, Fakin D, Kleinschek KS, Gorgieva S. Alkaline membrane fuel cells: Anion exchange membranes and fuels. *Sustain. Energy Fuels* **2021**, *5*, 604–637.
5. Chen N, Lee YM. Anion exchange polyelectrolytes for membranes and ionomers. *Prog. Polym. Sci.* **2021**, *113*, 101345.
6. Park EJ, Kim YS. Quaternized aryl ether-free polyaromatics for alkaline membrane fuel cells: synthesis, properties, and performance—A topical review. *J. Mater. Chem. A* **2018**, *6*, 15456–15477.

7. Mahmoud AMA, Miyatake K. Highly conductive and alkaline stable partially fluorinated anion exchange membranes for alkaline fuel cells: Effect of ammonium head groups. *J. Membr. Sci.* **2022**, *643*, 120072.

8. Chen N, Long C, Li Y, Lu C, Zhu H. Ultrastable and High Ion-Conducting Polyelectrolyte Based on Six-Membered N-Spirocyclic Ammonium for Hydroxide Exchange Membrane Fuel Cell Applications. *ACS Appl. Mater. Interfaces* **2018**, *10*, 15720–15732.

9. Park HJ, Chu XM, Kim SP, Choi D, Jung JW, Woo J, et al. Effect of N-cyclic cationic groups in poly(phenylene oxide)-based catalyst ionomer membranes for anion exchange membrane fuel cells. *J. Membr. Sci.* **2020**, *608*, 118183.

10. Chen N, Jin Y, Liu H, Hu C, Wu B, Xu S, et al. Insight into the alkaline stability of N-heterocyclic ammonium groups for anion-exchange polyelectrolytes. *Angew. Chem. Int. Ed. Engl.* **2021**, *60*, 19272–19280.

11. Mahmoud AMA, Miyatake K. Highly Conductive and Ultra Alkaline Stable Anion Exchange Membranes by Superacid-Promoted Polycondensation for Fuel Cells. *ACS Appl. Polym. Mater.* **2023**, *5*, 2243–2253.

12. Fan J, Willdorf-Cohen S, Schibli EM, Paula Z, Li W, Skalski TJG, et al. Poly(bis-arylimidazoliums) possessing high hydroxide ion exchange capacity and high alkaline stability. *Nat. Commun.* **2019**, *10*, 2306.

13. Xue B, Cui W, Zhou S, Zhang Q, Zheng J, Li S, et al. Facile Preparation of Highly Alkaline Stable Poly(arylene–imidazolium) Anion Exchange Membranes through an Ionized Monomer Strategy. *Macromolecules* **2021**, *54*, 2202–2212.

14. Hibbs MR. Alkaline stability of poly(phenylene)-based anion exchange membranes with various cations. *J. Polym. Sci. Part B: Polym. Phys.* **2013**, *51*, 1736–1742.

15. Pham TH, Olsson JS, Jannasch P. Effects of the N-alicyclic cation and backbone structures on the performance of poly(terphenyl)-based hydroxide exchange membranes. *J. Mater. Chem. A* **2019**, *7*, 15895–15906.

16. Lee WH, Mohanty AD, Bae C. Fluorene-based hydroxide ion conducting polymers for chemically stable anion exchange membrane fuel cells. *ACS Macro. Lett.* **2015**, *4*, 453–457.

17. Huang G, Mandal M, Peng X, Yang-Neyerlin AC, Pivovar BS, Mustain WE, et al. Composite Poly(norbornene) Anion Conducting Membranes for Achieving Durability, Water Management and High Power (3.4 W/cm^2) in Hydrogen/Oxygen Alkaline Fuel Cells. *J. Electrochem. Soc.* **2019**, *166*, F637.

18. Chen N, Long C, Li Y, Lu C, Zhu H. Ultrastable and High Ion-Conducting Polyelectrolyte Based on Six-Membered N-Spirocyclic Ammonium for Hydroxide Exchange Membrane Fuel Cell Applications. *ACS Appl. Mater. Interfaces* **2018**, *10*, 15720–15732.

19. Dang H-S, Jannasch P. Exploring Different Cationic Alkyl Side Chain Designs for Enhanced Alkaline Stability and Hydroxide Ion Conductivity of Anion-Exchange Membranes. *Macromolecules* **2015**, *48*, 5742–5751.

20. Mandal M, Huang G, Kohl P. A. Anionic multiblock copolymer membrane based on vinyl addition polymerization of norbornenes: Applications in anion-exchange membrane fuel cells. *J. Membr. Sci.* **2019**, *570*, 394–402.

21. Wang HH, Hu C, Park JH, Kim HM, Kang NY, Bae JY, et al. Reinforced poly(fluorenyl-co-terphenyl piperidinium) anion exchange membranes for fuel cells. *J. Membr. Sci.* **2022**, *644*, 120160.

22. Hu C, Park JH, Kim HM, Wang HH, Bae JY, Liu ML, et al. Robust and durable poly(aryl-co-aryl piperidinium) reinforced membranes for alkaline membrane fuel cells. *J. Mater. Chem. A* **2022**, *10*, 6587–6595.

23. Mahmoud AMA, Miyatake K. Tuning the Hydrophobic Component in Reinforced Poly(arylimidazolium)-Based Anion Exchange Membranes for Alkaline Fuel Cells. *ACS Appl. Energy Mater.* **2022**, *5*, 15211–15221.

24. Yamaguchi T, Nakao S, Kimura S. Plasma-graft filling polymerization: preparation of a new type of pervaporation membrane for organic liquid mixtures. *Macromolecules* **1991**, *24*, 5522–5527.

25. Ono H, Kimura T, Takano A, Asazawa K, Miyake J, Inukai J, et al. Robust anion conductive polymers containing perfluoroalkylene and pendant ammonium groups for high performance fuel cells. *J. Mater. Chem. A* **2017**, *5*, 24804–24812.

26. Miyake J, Taki R, Mochizuki T, Shimizu R, Akiyama R, Uchida M, Miyatake K. Design of flexible polyphenylene proton-conducting membrane for next-generation fuel cells. *Sci. Adv.* **2017**, *3*, eaao0476.

27. Mahmoud AMA, Miyatake K. Highly conductive and alkaline stable partially fluorinated anion exchange membranes for alkaline fuel cells: effect of ammonium head groups. *J. Membr. Sci.* **2022**, *643*, 120072.

28. Ikawa M, Yamada T, Matsui H, Minemawari H, Tsutsumi J, Horii Y, et al. Simple push coating of polymer thin-film transistors. *Nat. Commun.* **2012**, *3*, 1176.

29. Otsuji K, Yokota N, Tryk DA, Kakinuma K, Miyatake K, Uchida M. Performance hysteresis phenomena of anion exchange membrane fuel cells using an Fe–N–C cathode catalyst and an in-house-developed polymer electrolyte. *J. Power Sources* **2021**, *487*, 229407.